

Supporting Information

Stable and efficient phosphorescent organic light-emitting device utilizing δ -carboline-containing thermally activated delayed fluorescence host

Hui Wang,^a Hongyu Zhao,^b Chunxiu Zang,^a Shihao Liu,^a Letian Zhang,^{a*} Wenfa Xie^{a*}

^aState Key Laboratory of Integrated Optoelectronics, College of Electronic Science and Engineering, Jilin University, Changchun, 130012, People's Republic of China.

^bBeijing Tuocai Optoelectronics Technology CO. LTD, Beijing, 100086, People's Republic of China.

*E-mail: zlt@jlu.edu.cn, xiewf@jlu.edu.cn

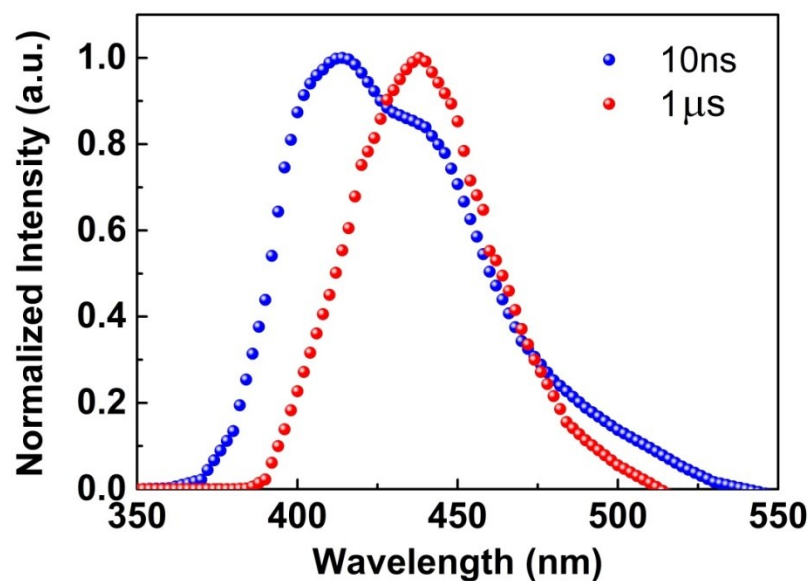


Figure S1. Prompt and delayed spectra at 10 ns and 1 μ s.

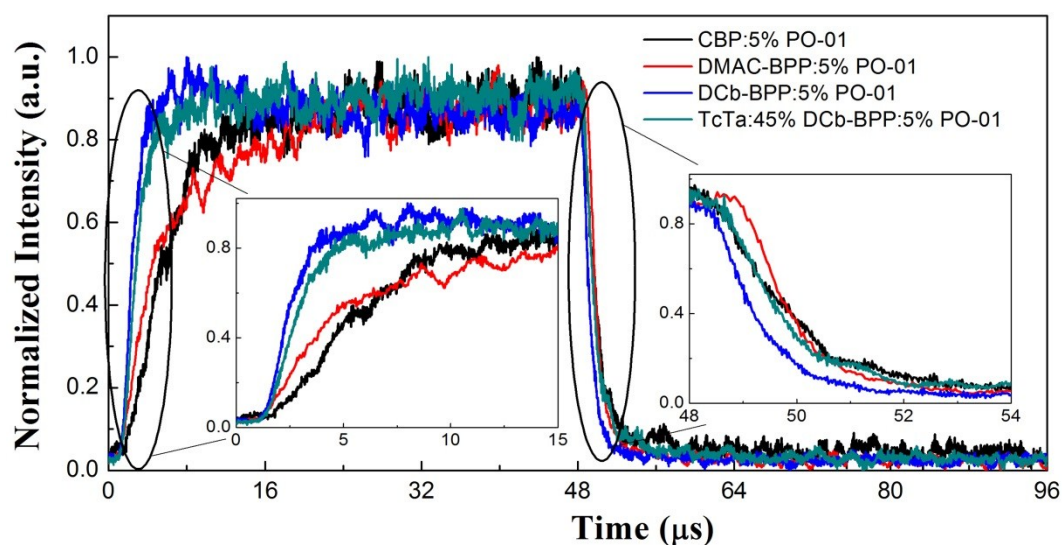


Figure S2. Transient EL curves of the devices observed at 560 nm. Inset: (left) the turn-on process, (right) cut-off process.

The power source is a rectangular wave with high level of 6 V and low level of 0 V, period of 96 μs , and duty cycle of 50%. Device 1 has the slowest turn-on process, which can be attributed to the lower mobility of CBP. Device 3 has a narrow recombination area and high mobility, causing the fastest turn-on process by accumulated excitons. This result also accords with the lowest turn-on voltage of device 3.

At the cut-off state, it can be seen that all the devices have a delay compared with the electrical signal (turn off @ 48 μs). Obviously, the delayed emission of the device 3 is the first to disappear and its decay tendency is also the fastest, because of the narrow recombination region and the faster excitons emission. So, there is almost no residual exciton after cut off the electrical excitation. Because the prompt lifetime of DMAC-BPP (43 ns) is much longer than DCb-BPP (4.2 ns), the rate of FRET in device 3 is much higher than device 2 under the same concentration. Compared with device 3, the delayed emission of device 4 is longer, due to the balanced carrier transporting. The fitted EL decay lifetimes are 1.63 μs , 0.91 μs , 0.86 μs , and 1.06 μs , respectively.

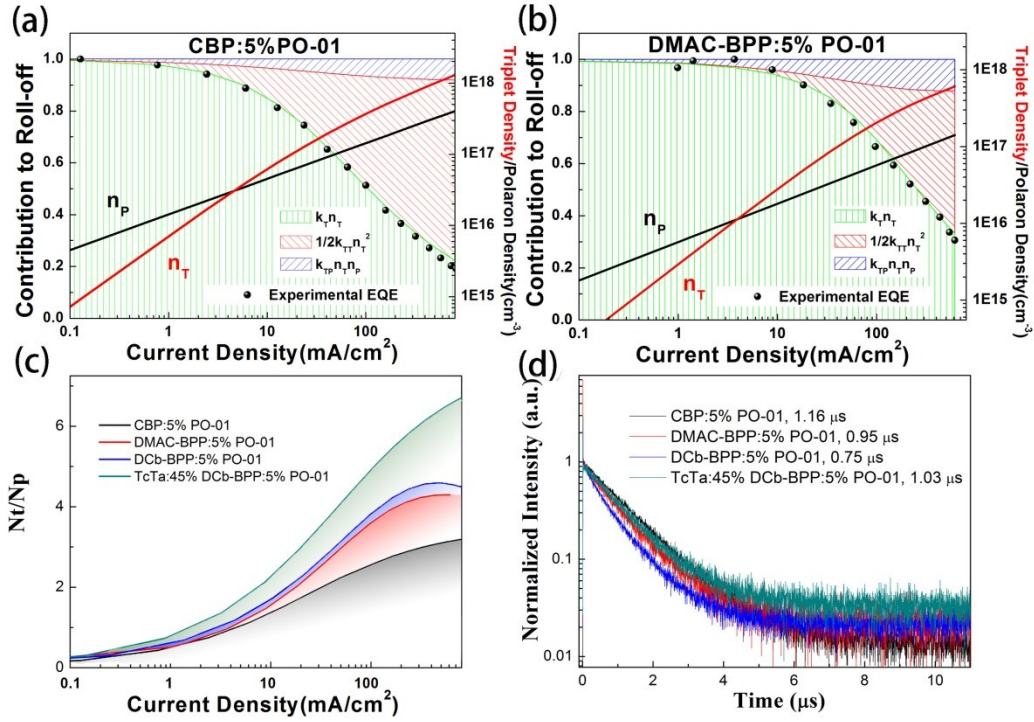


Figure S3. Simulated IQE, TTA, TPA, triplet density (N_t), and polaron density (N_p) plotted with current density for the (a-d) device 1-4. (e) The ratio of triplet and polaron density (N_t/N_p) in devices. (f) PL decay of emissive layers in device 1-4.

To investigate the effect of the annihilation process, mainly contain triplet-triplet annihilation (TTA) and triplet-polaron annihilation (TPA), on efficiency roll-off of PHOLEDs, we simulated the contribution of the TTA and TPA to efficiency loss in PHOLED by solving the rate equations for the triplet and polaron density. We use the simplified equation to simulate the occupation of the effective emission and annihilations. The triplet density/polaron density (N_t/N_p) reflects the proportion of triplet to some degree.

As is shown in Figure S2a, the annihilation in device 1 contains more TTA, reflecting a small N_t/N_p . The small ratio means that the plenty of triplet-involved annihilations occurred in device 1 consuming triplet. In device 3, the most of annihilation is caused by TPA, related to the high current density. Device 4 has the highest N_t/N_p , demonstrating device 4 contains more triplets to emit. That is why device 4 is the most efficient device.

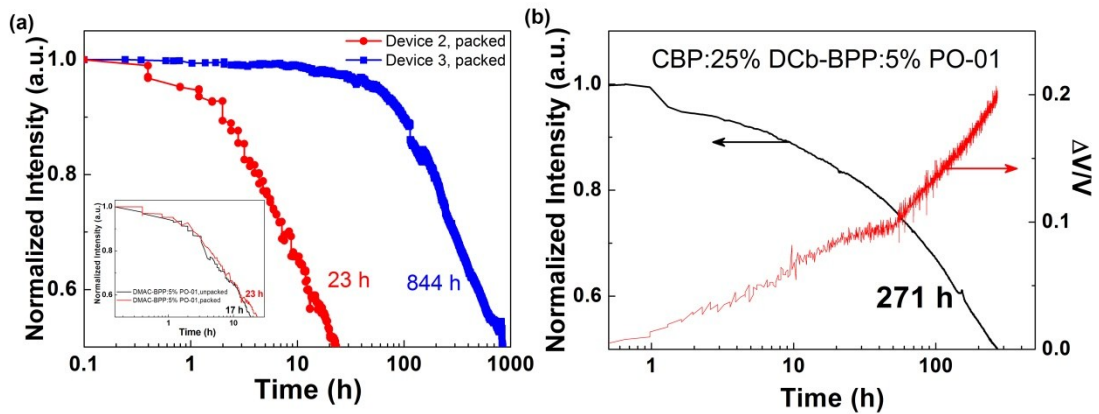


Figure S4. (a) Luminescence with time of Device 2 and Device 3 with simple packages. (Inset) Luminescence with time of Device 2 with and without package. (b) Luminescence with time of devices with EML of CBP:25%DCb-BPP:5%PO-01 in the air without any protection, $L_0=1000 \text{ cd/m}^2$. And the change in voltage relative to the initial value with time

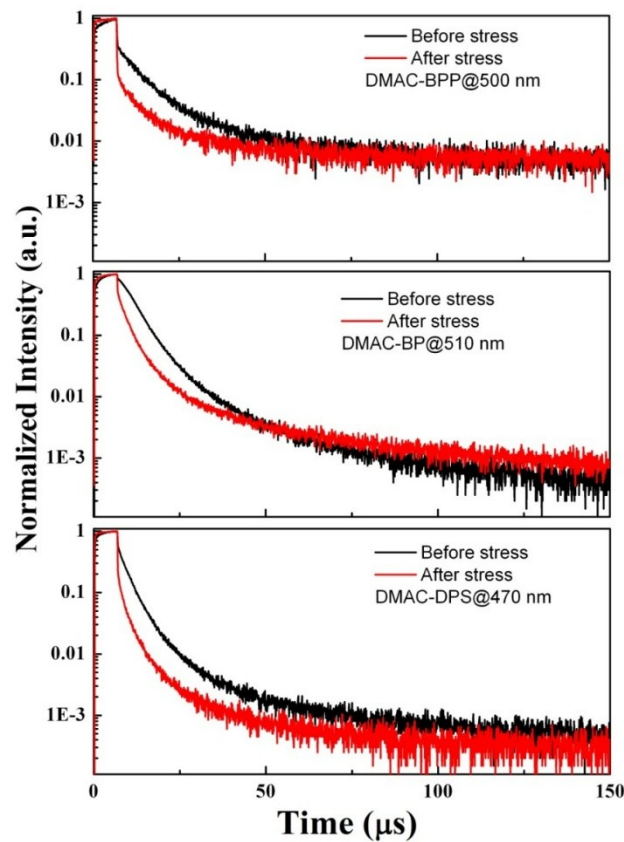


Figure S5. Transient decay spectra of nondoped devices with EML of DMAC-BPP, DMAC-BP, and DMAC-DPS for before and after stress.